TOPICAL REVIEW — Low-dimensional nanostructures and devices

Graphene applications in electronic and optoelectronic devices and circuits

Wu Hua-Qiang(吴华强)[a)b)†], Linghu Chang-Yang(令狐昌洋)[a)], Lü Hong-Ming(吕宏鸣)[a)], and Qian He(钱 鹤)[a)b)]

[a)] *Institute of Microelectronics, Tsinghua University, Beijing* 100084, *China*

[b)] *Tsinghua National Laboratory for Information Science and Technology* (*TNList*), *Beijing* 100084, *China*

(Received 27 July 2013; revised manuscript received 15 August 2013)

Recent progress of research for graphene applications in electronic and optoelectronic devices is reviewed, and recent developments in circuits based on graphene devices are summarized. The bandgap–mobility tradeoff inevitably constrains the application of graphene for the conventional field-effect transistor (FET) devices in digital applications. However, this shortcoming has not dampened the enthusiasm of the research community toward graphene electronics. Aside from high mobility, graphene offers numerous other amazing electrical, optical, thermal, and mechanical properties that continually motivate innovations.

Keywords: graphene, electronic device, optoelectronic device, circuit

PACS: 81.05.ue **DOI:** 10.1088/1674-1056/22/9/098106

1. Introduction

Two-dimensional material systems have attracted great attention in global research communities. Graphene is a two-dimensional material with only one-atom thickness. It combines unique electronic properties (e.g., exceptionally high mobility), extreme mechanical strength, and excellent thermal conductivity. Graphene based electronic devices have quickly emerged as promising candidates for post-silicon technology. Its remarkable optical properties may enable many new applications in optoelectronics.

In October 2004, researchers at the University of Manchester successfully prepared single-layer graphene through mechanical exfoliation and demonstrated an electric field effect in the sample,[1] igniting enthusiastic worldwide pursuit of graphene electronics.

Graphene is a flat monolayer of carbon atoms tightly packed into a two-dimensional honeycomb lattice. Each carbon atom is covalently bonded with three nearest carbon atoms through sp^2 hybridization, with the remaining p_z carbon orbitals forming an extended electron system. The conduction and valence bands touch at the corners of the Brillouin Zone, the touch points are called the Dirac points. For low carrier energies, which are dominant in electron transport, the bands feature a linear dispersion $E = v_F hk$, where v_F represents the Fermi velocity and is about 1/300 of the speed of light. This linear relation indicates that the electrons are massless. Because it lacks a bandgap, graphene is described as a semimetal. The density of states (DOS) increases linearly with energy, which differs from that in the conventional two-dimensional electron gas (2DEG).

Graphene has excellent mechanical, thermal, and electrical properties:

- a Young's modulus of 1 TPa and intrinsic strength of 130 GPa;[2]
- very high thermal conductivity, above 3000 $W \cdot mK^{-1}$;[3]
- impermeability to any gas;[4]
- very high electron mobility, $\sim 200000\ cm^2 \cdot V^{-1} \cdot s^{-1}$ (in suspended graphene).[5]

Due to its extremely high mobility, graphene is considered a promising material for ultra-high speed electronics, including digital logic, analog circuits (e.g., radio-frequency amplifiers and mixers) and interconnects. Since monolayer graphene is a gapless material, graphene transistors show poor intrinsic gains and low on-off ratios in recent reports,[6,7] making them unsuitable for digital logic applications. However, graphene-based electronic devices and circuits are still considered excellent candidates for radio-frequency (RF) applications where switching off the transistors is unnecessary.[8] Analog electronics has become a primary target application for graphene devices.

Graphene also possesses remarkable optical properties. It absorbs a constant ($\pi a = 2.3\%$) fraction of incident white light.[9] The linear dispersion of the Dirac electrons enables graphene based optoelectronic devices for broadband applications. The saturable absorption is achieved as a consequence of Pauli blocking. Other intriguing properties include high optical damage threshold and high third-order optical nonlinearities. These properties inspire many photonic device applications.

Many good review papers summarize recent progress in graphene research, from material synthesis and properties to

†Corresponding author. E-mail: wuhq@mail.tsinghua.edu.cn

© 2013 Chinese Physical Society and IOP Publishing Ltd

transistors and novel electronics.[10–12] In this review, the applications of graphene in the field of electronic and optoelectronic devices are discussed and recent developments in circuits based on graphene devices are summarized.

2. Material preparation

High quality graphene can readily be obtained through mechanical exfoliation from highly oriented pyrolytic graphite (HOPG).[1] This discovery expedites graphene research since it makes obtaining high quality graphene samples relatively easy. Many basic researches have been conducted on such exfoliated graphene layers. However, for industrial applications of graphene, it is necessary to develop synthesis methods capable of producing well-controlled, large-scale, high-quality graphene. Currently, there are two major methods of growing large scale graphene. The first is the epitaxy growth and is based on the thermal decomposition of SiC.[13,14] By heating SiC wafers to around 1500 °C, Si desorbs and the remaining carbon reforms into a graphene layer.[15,16] This method is limited by the size of available SiC wafers and the high cost of SiC substrates.

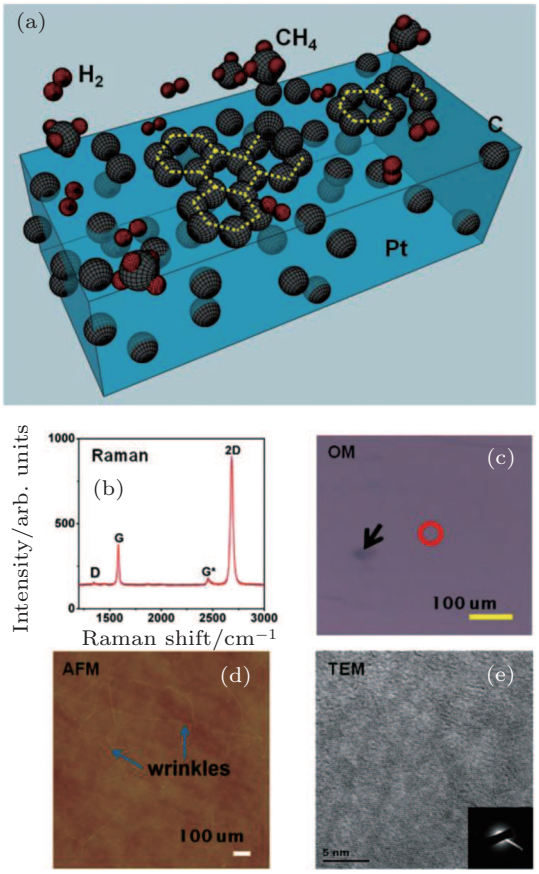


Fig. 1. High quality monolayer graphene growth through atmospheric pressure CVD method on Pt foil. (a) Mechanism of graphene growth on Pt foil. (b) Raman spectra, (c) optical microscope image, (d) AFM image, (e) TEM image.[22]

The other widely used synthesis method is chemical vapor deposition (CVD) growth on metals such as Ru,[17] Ni,[18] Cu,[19,20] and Pt.[21,22] In particular, CVD growth on Pt has recently attracted increasing attention. Platinum has a low carbon solubility, a high melting temperature, and a low thermal expansion coefficient, and it is also inert to oxidation. These properties give the Pt substrate a more stable surface morphology during the high temperature CVD growth process and make Pt a suitable substrate for single-layer graphene growth as shown in Fig. 1. Graphene grown on Pt or Cu foil can be transferred to any substrate for device fabrication.

3. Transfer of graphene films

Once graphene films are grown on a metal by CVD synthesis method, they are ready to be transferred to the target substrate for further device fabrication. For transferring graphene from the inert metals, such as Pt, a 'bubbling transfer process' is preferred.[23] For transferring graphene from the reactive metals, like Cu, Ni, and Ru, transfer by etching the metals away is preferred.[24]

In both cases, a layer of organic polymer film, commonly polymethyl-methacrylate (PMMA), should be coated on the graphene first. The resulting PMMA/graphene film has much greater mechanical strength than the graphene film alone and can also help protect the graphene film during the transfer process. In the bubbling transfer process, the PMMA/graphene/Pt plate is used as a cathode, with another Pt foil used as an anode. To perform the water reduction reaction, both electrodes are dipped into a NaOH aqueous solution and connected to a power source with a constant current supply. Then the PMMA/graphene film will gradually be separated from the Pt plate driven by the H_2 gas bubbles generated at the cathode. In the final step of the transfer process, the washed PMMA/graphene film is placed on the target substrate, and the PMMA layer is removed by acetone. In contrast, for transfer by metal etching, the PMMA/graphene/metal plate is dipped into an etching solution to etch the metal away. Then the PMMA/graphene film is washed and placed on the target substrate. At this step, the PMMA film can be removed directly by acetone, but recently, researchers[24] obtained better transfer quality when they deposited a second layer of PMMA on the existing PMMA film and cured the sample at 180 °C for about 1 min before removing the PMMA from the graphene.

4. Graphene electronics

4.1. RF FETs

Graphene is an excellent channel material for devices in radio-frequency applications. First of all, its ultra-high mobility, which leads to micrometer-scale ballistic transport, together with very large saturation velocity, brings graphene enormous potential for high-frequency devices. In addition, the outstanding thermal conductivity and micrometer-scale ballistic transport inspire great hope for using graphene in low-noise amplifiers.[25,26]

The most important measures for RF transistors are two characteristic frequencies: the cutoff frequency, f_T, at which the small-signal current gain decreases to unity, and the maximum frequency of oscillation, f_{max}, at which the unilateral power gain drops to unity. Figure 2 shows recently reported cutoff frequencies of graphene field-effect transistors (FETs) versus the device gate length, compared to Si MOSFETs and III–V high-electron-mobility transistors (HEMTs). Currently, the highest f_T reported for graphene FETs is 427 GHz,[27] while the highest f_{max} is only 45 GHz.[6] The low f_{max} performance is due to the gapless nature of graphene, which leads to large source/drain series resistances, weak current saturation, and ambipolar conduction.[8]

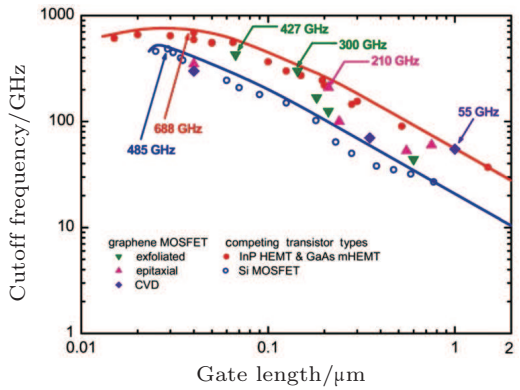


Fig. 2. Cutoff frequency f_T of graphene MOSFETs, Si MOSFETs, and III–V HEMTs (InP HEMTs and GaAs mHEMTs) versus gate length.[8]

The field effect in graphene was investigated right after the first Scotch tape-enabled isolation of the material. In that report (2004), the exfoliated graphene was transferred onto a dielectric layer of 300-nm thick SiO_2, and a heavily doped n-type silicon wafer under the SiO_2 layer was used as a back gate. The observed device behavior was similar to the ambipolar field effect in semiconductors. The first top-gated graphene FET (GFET) was realized in 2007 by Lemme,[28] with a 500-nm gate length. Since then, significant progress in RF GFET research has been made. In 2008, Meric[29] achieved the first gigahertz GFET, with f_T over 14.7 GHz and a 500-nm gate length. He also proved that the current gain in the GFET followed a $1/f$ dependence on the frequency, similar to semiconductor RF devices, sparking the development of high-frequency GFETs. Later in the same year, IBM reported a 26-GHz-f_T GFET, using exfoliated graphene with a gate length as short as 150 nm, demonstrating that the f_T performance could be improved by decreasing the gate length.[30] In 2009, HP research laboratory realized the first epitaxial-GFET on SiC substrate, with a 2-μm gate length and 4.4 GHz f_T.[31] By using epitaxial graphene grown directly on the substrate, they proved that epitaxial GFETs, unlike GFETs using exfoliated graphene, could be fabricated with relatively large scale integration. In 2010, IBM pushed the frontline of f_T further to 100 GHz by using an epitaxial GFET on SiC with a 240-nm gate length.[32] This was a big step forward, since the f_T of the GFET, which was fabricated through an integrated process, was comparable to that of a semiconductor RF device with the same gate length. In the same year, Duan's group at UCLA achieved a GFET with an f_T of 300 GHz, using a self-aligned nanowire as the gate.[33] By precisely positioning the source, the drain, and the nanowire gate through a self-alignment process, the source/drain series resistances as well as the parasitic capacitance were greatly reduced, resulting in outstanding device RF performance. Using CVD graphene, IBM realized a 155-GHz GFET on a diamond-like carbon substrate with a deep submicrometer gate length as short as 40 nm in 2011.[34] In their work, they also demonstrated the scaling behavior of the device cut-off frequencies with the gate length down to 40 nm. In 2012, Duan's group reported a GFET with transferred gate stacks and a record-high 427 GHz f_T.[27] The gate stacks of the device were first fabricated independently and then transferred to a SiO_2 substrate with patterned CVD graphene on top. This unique process avoided introducing undesired damage or impurities into the graphene lattice, and further reduced the excessive parasitic capacitance or serial resistances. In summary, the development of RF GFET performance depends mainly on improving the source/drain resistance by introducing defects in graphene contacts;[35] suppressing the surface phonon scattering in graphene channels by choosing proper substrates, dielectrics (h-BN dielectrics[36]), and fabrication process (widely-used atomic layer deposition process of Al_2O_3 dielectrics[37]); and reducing the parasitic capacitance by scaling down the device.[26] Table 1 summarizes recent research progresses of GFET in f_T improvement.

Table 1. Research progress summary of RF GFETs.

Achievement	Gate length/nm	f_T/GHz	Publication date	Reference
Field-effect in graphene	–	–	Oct. 2004	[1]
First top-gated GFET	500	–	April 2007	[23]
First gigahertz GFET	500	14.7	Dec. 2008	[24]
First GFET with submicrometer gate length	150	26	Dec. 2008	[25]
First epitaxial GFET on SiC	2000	4.4	May 2009	[26]
First 100 GHz epitaxial GFET on SiC	240	100	Feb. 2010	[27]
First nanowire gate GFET	144	300	Sep. 2010	[28]
First CVD GFET with deep submicrometer gate length	40	155	April 2011	[29]
First 427 GHz GFET with transferred gate stacks	67	427	July 2012	[22]

4.2. Logic applications

In either logic or analog applications, transistors must have high enough power gains to drive the next stage. Unlike the traditional semiconductors, graphene is a gapless material, and GFETs lack sufficient intrinsic gains. Although the recent progress is far from meeting the demands of logic applications, numerous approaches have been explored to increase the intrinsic gain of GFET, e.g., increasing the gate control to introduce the minimal density point to the channel for current saturation,[38] new device structure for full channel gating,[39] layout design of multiple-finger devices,[40] etc.

Recently, an integrated GFET ring oscillator reportedly achieved the highest frequency (1.28 GHz) among ring oscillators using low-dimensional material transistors, with a 0.57 V output voltage swing,[41] as shown in Fig. 3. Ring oscillators are commonly used to evaluate the performance of digital technology. Made by a fabrication process similar to that of devices in Ref. [39], they reduced the parasitic capacitances in devices and circuits, suggesting further improvements are possible to make the GFETs suitable for logic applications.

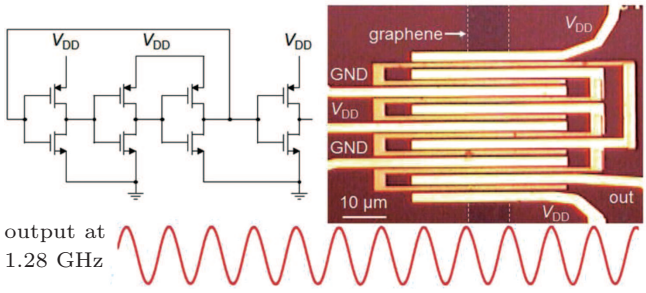


Fig. 3. Circuit diagram and chip image of integrated GFET ring oscillators.[41]

4.3. Vertical devices

Recently, vertical graphene transistors based on tunneling transport instead of the classical MOSFET principle are investigated.[42] In that work, a so-called BiSFET (bilayer pseudo-spin field-effect transistor) utilizes the exciton condensation to modulate inter-layer tunneling in bi-layer graphene devices, which in principle could achieve ultra-low switching energy. However, the vertical tunneling graphene transistors still face various challenges, e.g., fabrication complexity, low drain current ($\sim$ 10 pA/μm), etc.

4.4. Amplifiers

For high frequency (GHz) amplifier applications, several common-source GFET amplifiers have been investigated. In Han's work,[40] a 6-finger embedded-gate GFET common-source amplifier, with 500 nm gate length in each finger, exhibited 5 dB low frequency gain with the 3 dB bandwidth greater than 6 GHz, see Fig. 4. The current saturation was achieved by an embedded gate structure with deeply scaled 4-nm HfO_2 gate oxide. IBM researchers achieved a top gated GFET amplifier on an SiC substrate,[6] as shown in Fig. 5, which is more feasible for integration with other elements in a complete circuit. The maximum voltage gain for a 1.5 μm device at 5 MHz is 3 dB.

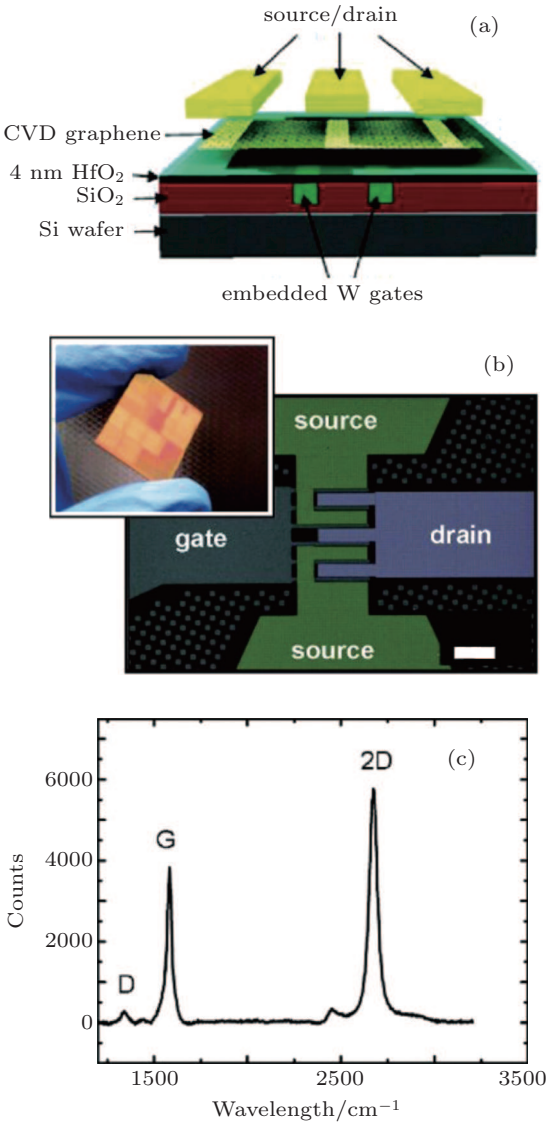


Fig. 4. (a) Schematic diagram of the embedded gate structure. CVD graphene pieces were transferred onto an 8 in. wafer with pre-patterned metal gates covered by a high quality high-k dielectric. (b) Scanning electron microscope image of a 6-finger device with 500 nm gate length. Inset shows photograph of a finished die (with graphene piece) fabricated in a Si-fab. (c) Raman spectrum of CVD-grown graphene.[40]

For low frequency amplifier applications (kHz), the structure of complementary inverters is preferred to increase the voltage gain. As shown in Fig. 6, the top gate of the GFET device overlaps the source/drain contacts, resulting in full-channel gating and high voltage gain.[39,43]

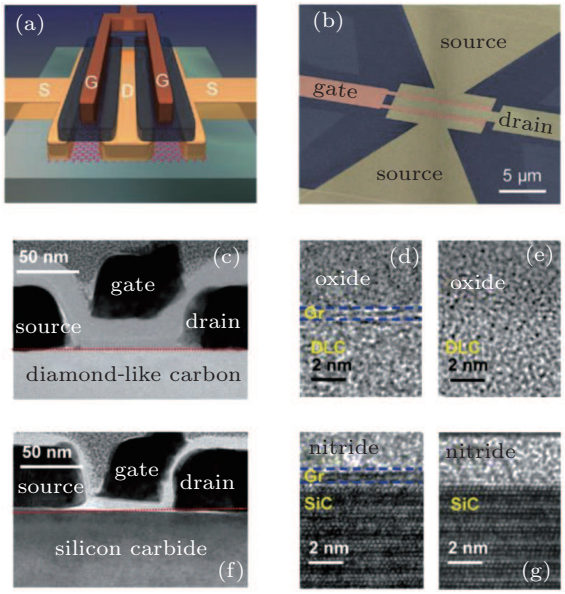


Fig. 5. Schematic diagram and electron images of graphene RF transistors. (a) Schematic diagram of a top-gated graphene RF transistor on a DLC substrate. (b) SEM image of a typical top-gated dual-channel RF device. The scale bar is 5 μm. (c) Cross-section TEM image of a transistor based on CVD graphene on DLC; (d) and (e) the high-resolution TEM images of the channel region of an active device and an open device where graphene is etched away, respectively. (f) Cross-section TEM image of a transistor based on epitaxial graphene on SiC; (g) and (h) the high-resolution TEM images of the channel region of an active device and an open device where graphene is etched away, respectively. In panels (c) and (f), the scale bar is 50 nm. In panels (d), (e), (g), and (h), the scale bar is 2 nm.[6]

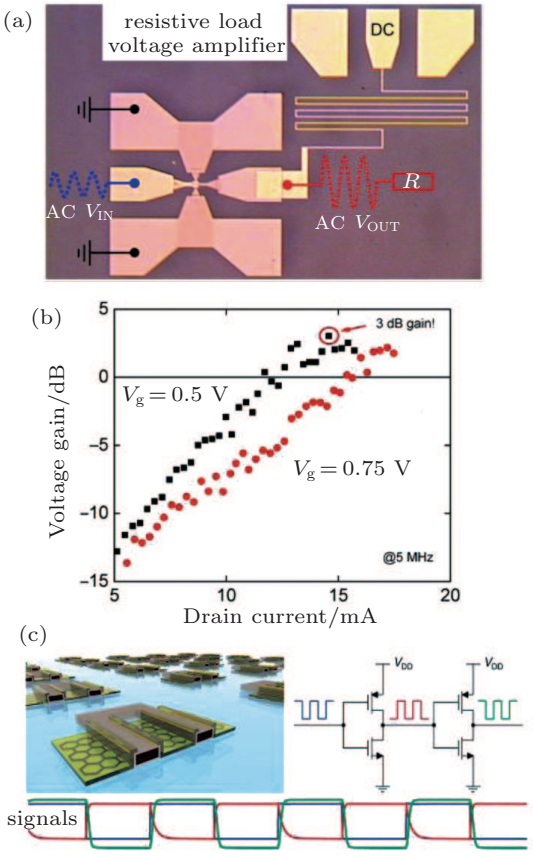


Fig. 6. Integrated graphene complementary inverters. (a) Schematic diagram of a large array of inverters fabricated on wafer-scale graphene. (b) Circuit diagram of two cascaded inverters. (c) Digital waveforms measured under ambient conditions in a cascade connection of two graphene inverters.[39]

4.5. Mixer

Mixers are core components in RF front end to produce signals at the sum and difference of the two input frequencies. Most of the recent approaches are focused on two types of graphene mixers: ambipolar mixer and resistive drain mixer. The ambipolar mixer utilizes the symmetrical ambipolar-transport characteristic of GFET for nonlinear mixing, where the characteristic usually contains a large quadratic component. The first GFET ambipolar mixer was realized by Wang *et al.* in 2010.[44] The mixer operated at a fundamental frequency of 10 MHz with a 35 dB conversion loss, as shown in Fig. 7. Due to the chemical doping-induced asymmetry, induced by impurities in the ambipolar-transport characteristic, the unwanted third-order components in the mixer output signal were relatively large.

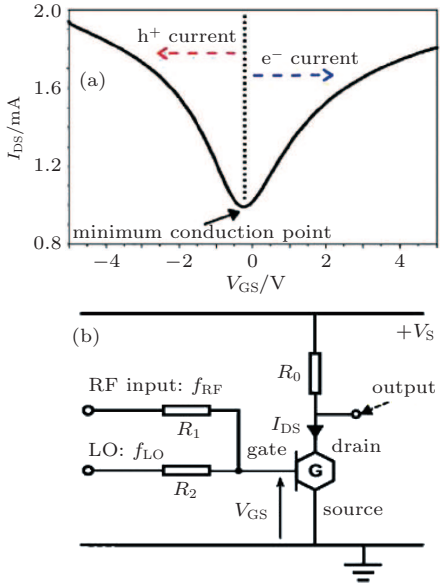


Fig. 7. (a) The drain–source current versus gate–source voltage (I_D–V_{GS}) characteristic of fabricated GFETs with $L_G = 2$ μm, $W_G = 2 \times 75$ μm, and $L_{DS} = 5$ μm. The minimum conduction point is very close to 0 V. (b) Proposed circuit for graphene ambipolar RF mixers. Note: no DC bias is needed at the input due to the minimum conduction point being close to 0 V.[44]

A resistive drain mixer uses the linear output characteristic of GFET for mixing, where the GFET is biased as a unipolar FET. In 2011, Lin *et al.* presented the first resistive drain mixer, operating at 4 GHz and with a 27 dB conversion loss.[45] In their work, the unwanted high order components in the mixer output signal were relatively smaller than those in Wang's ambipolar mixer, while the LO noise and RF feedthrough in the output signal were still significant. Early this year, Moon *et al.* achieved a zero-bias linear resistive drain GFET mixer at 20 GHz with a conversion loss as low as 14 dB,[46] see Fig. 8. Note that passive and linear mixers are preferred in RF communications for low intermodulation and low noise, since the inter-modulation performance of a receiver front end is often limited by that of the mixer.[47]

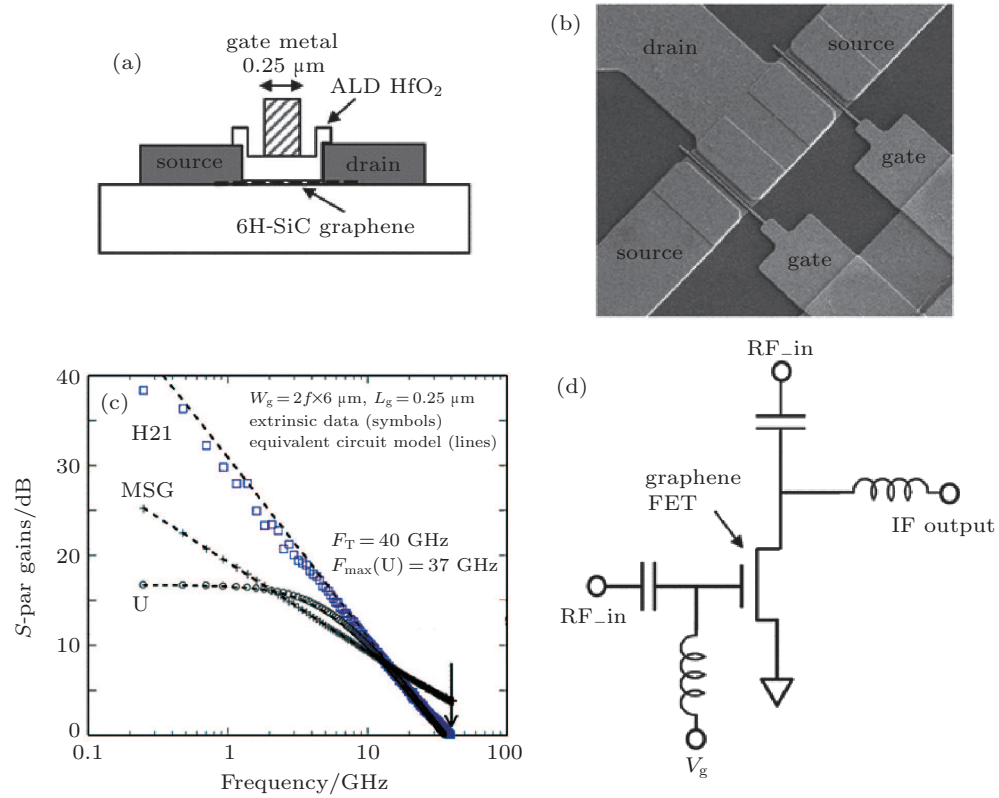


Fig. 8. (a) Schematic diagram of a top-gated HfO_2/graphene FET with a gate length of 0.25 μm. (b) SEM photograph of a two-gate-finger 6-μm-wide graphene FET (denoted as $2f \times 6$ μm). (c) Measured (without de-embedding) small-signal S-parameter gains of a graphene FET, along with an equivalent circuit model at $V_{ds} = 2$ V and $V_{gs} = -2.5$ V. (d) Schematic diagram of a resistive FET mixer, where the LO signal is applied to the gate (gate-pumped). The IF signal is measured at the drain. No impedance tuning is included.[46]

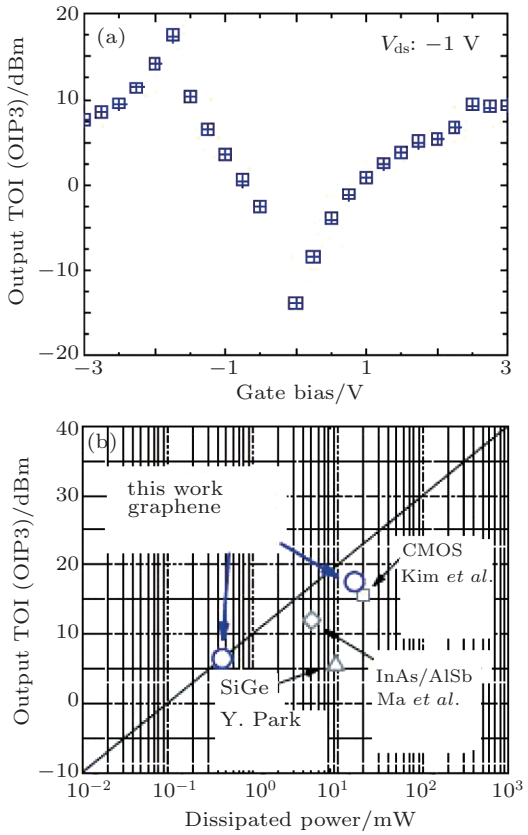


Fig. 9. Graphene transistors exhibit excellent linearity compared to conventional transistors. (a) Plot showing the dependency of the third order intercept on gate bias. (b) TOI versus DC dissipated power, showing graphene FET approaching (OIP3$>10\times$dissipated power).[48]

In 2012, Madan *et al.* made a comparison between an ambipolar mixer and a resistive drain mixer with an improved GFET fabrication process for highly scaled dielectric equivalent oxide thickness (EOT) and low source/drain contact resistance,[48] as shown in Fig. 9. They concluded that ambipolar gate mixing suppresses odd-order harmonics and outperforms resistive drain mixing. It is expected that improved performance may be achieved through further reducing the interface state density and scaling the EOT. It is hoped that the graphene based ambipolar mixer may become competitive with the conventional Gilbert cell mixers. In the same year, Omid *et al.* combined an ambipolar mixer and a resistive drain mixer by using the ambipolar-transport characteristic of GFET to double the LO frequency and then utilizing filters to couple the RF signal for resistive drain mixing.[49] They reported a so-called sub-harmonic mixer with a 24 dB conversion loss and a 2 GHz LO frequency. In that work, the LO noise was suppressed, and the separation of LO and RF was simplified with a wide frequency gap in between.

Recently, Zhu *et al.* proposed a four-GFET double-balanced passive mixer, with a topology similar to that commonly used in MOSFET mixers.[50] As shown in Fig. 10, the proposed device demonstrates high performance, good linearity, and no input frequency penetration in simulation, com-

pared to the ordinary MOSFET mixers and recent results from single-GFET mixers. Each of the four GFETs is biased as a resistive type mixer, and the unwanted higher order frequencies in the output are cancelled out. This mixer is highly compact to current receiver front end and can be fully integrated since there is no external component, in contrast to single GFET mixers.

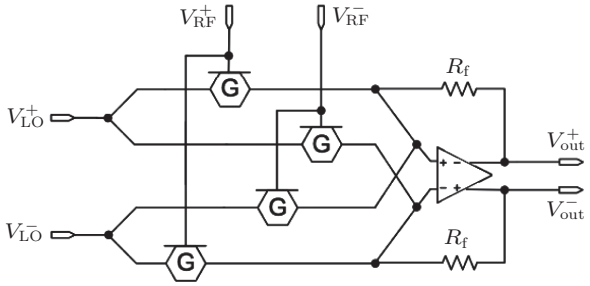


Fig. 10. Schematic diagram of four-GFET double-balanced mixer.[50]

In flexible electronics, the conventional FETs based on organic materials have poor mobility at about 1 $cm^2 \cdot V^{-1} \cdot s^{-1}$, while a flexible graphene FET can has a mobility as high as 3000 $cm^2 \cdot V^{-1} \cdot s^{-1}$. Lee *et al.* achieved an all-graphene QPSK transmitter on a flexible substrate operating at $\sim$ 10 kHz, in which the mixers were realized by ambipolar mixing and resistive drain mixing respectively.[51]

4.6. Interconnects

In large scale integrated circuits and systems, interconnects have become more and more critical for chip performance. When used as interconnects, graphene also shows a great potential. Theoretical calculations have shown that the conductivity of metallic graphene nanoribbons (GNR) would outperform copper wires with unity aspect ratio when the interconnect width is scaled down to below 8 nm.[52] The theory also predicts that high-quality doped GNRs offer smaller signal delay than copper at the 11 nm technology node when used as global wires. DC experimental characterizations show that the resistivity of good-quality GNRs in the width range from 18 nm to 50 nm is less than 10 $\mu\Omega \cdot$cm, which is comparable with copper wires with the same physical dimensions. Furthermore, GNRs have a breakdown current density on the order of 10^8 A/cm^2, which is ten times higher than the maximum possible current density of copper. However, despite the favorable theoretical and DC characterization results of graphene interconnects, the experimental demonstration of high speed signaling using graphene interconnects has not yet been realized, and there is no report of the integration of graphene with the standard CMOS technology, which is a key requirement for future integrated graphene electronics.[53]

5. Graphene optoelectronics

Besides the varied progress made in electronics fields, graphene also has wide applications in optoelectronics, such as photodetector, optical modulator, mode-locked laser, and optical polarizer.

5.1. Photodetector

A photodetector measures the photon flux or optical power by converting the energy of the absorbed photons into electrical signals. The conventional semiconductor photodetectors suffer from narrow detecting spectral ranges and maximum bandwidths limited by the carrier transit time. In contrast, the wavelength-independent absorption property of graphene enables its application in a wide spectral range from ultraviolet to infrared. In addition, the photo-generated carriers can be extracted at an ultrafast speed owing to the high carrier mobility. Xia *et al.* demonstrated an ultrafast photodetector with an intrinsic bandwidth over 500 GHz.[54] Moreover, the transit time limited bandwidth of graphene photodetectors is calculated to be 1.5 THz.[38]

The major obstacle of graphene photodetectors is low sensitivity due to the small detection area and the thinness of graphene. Two effective approaches to improve the graphene photodetectors' sensitivity are the introduction of a plasmonic nanostructure[55] and the integration with a waveguide,[56] as shown in Figs. 11 and 12. Pospischil *et al.*[57] recently demonstrated a CMOS-integrated graphene photodetector with a sensitivity of 0.05 A/W and a footprint of 50 μm^2.

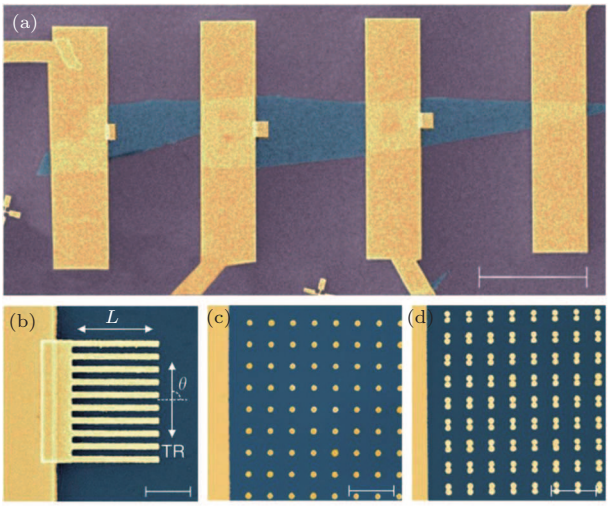


Fig. 11. Scanning electron microscopy micrographs of the graphene devices with plasmonic nanostructures. (a) An overall image of one such device. Blue, graphene; purple, SiO_2 (300 nm); yellow, Ti/Au electrodes. The scale bar is 20 μm. (b)–(d) Blow up of contacts with various tested plasmonic nanostructures. The scale bar is 1 μm.[55]

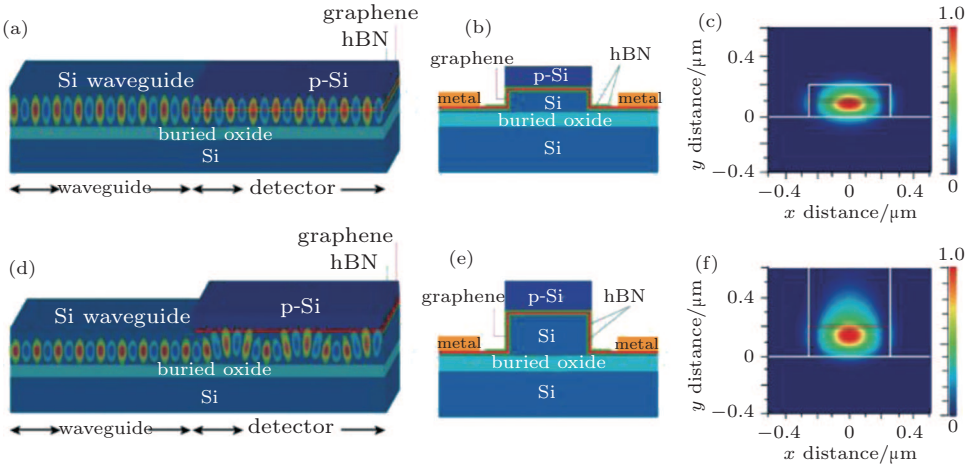


Fig. 12. The structure of graphene photodetectors with integrated waveguides. (a)–(c) Butt-coupled photodetectors. (d)–(f) Evanescent-coupled photodetectors.[56]

5.2. Optical modulator

Due to their weak electro-optical properties, Si modulators' footprint is on the order of millimeters.[58] Moreover, those devices suffer from narrow operation spectra and slow switching time. Germanium and compound semiconductors, on the other hand, face problems of integration with existing Si platforms.[59] With their ability to absorb the incident light over ultra-wide spectra and ultrafast response, graphene optical modulators can achieve excellent performance. By tuning graphene's Fermi level electrically, the inter-band transitions of photo-generated electrons can be modulated. Liu *et al.* demonstrated the modulation of the guided light at frequencies over 1 GHz, covering a broad operating spectrum in near infrared range,[60] as shown in Fig. 13. The modulation can also be based on the intra-band transition in graphene. A transmissive surface plasmon modulator has been demonstrated by Anderson *et al.*, which worked in a long-wavelength infrared range. The graphene Fermi level was modulated by a back gate.[61]

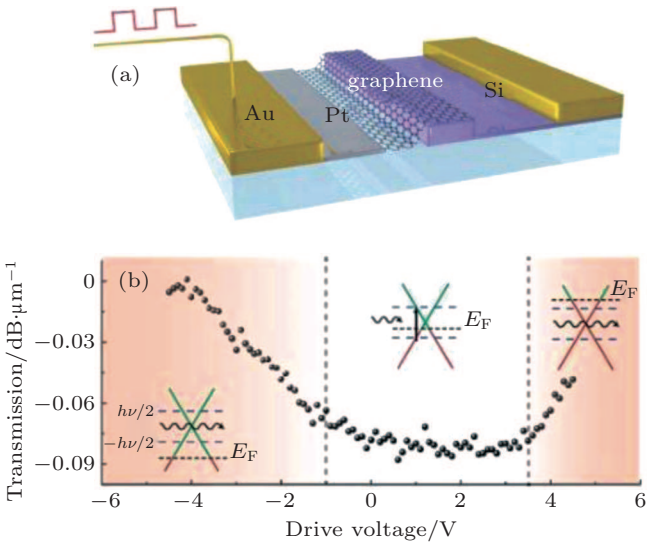


Fig. 13. (a) Three-dimensional schematic illustration of the device; a monolayer graphene sheet is on the top of a silicon bus waveguide, separated from it by a 7-nm-thick Al_2O_3 layer. (b) Static electro-optical response of the device at different drive voltages.[60]

5.3. Mode-locked laser

Mode-locked lasers have been used in various applications, such as material micromachining,[62] bio-medicine,[63] spectroscopy, and so forth. A semiconductor saturable absorber mirror (SESAM), as the most common mode locking element, has drawbacks of low damage threshold, narrow absorption wavelength range, and lying inside the visible and near-infrared regions. Also, its fabrication requires costly complex epitaxial growth techniques. In contrast, graphene-based saturable absorbers have the advantages of ultrafast carrier relaxation time, strong absorption, controllable modulation depth, wide spectral range tenability,[64] and high thermal conductivity.

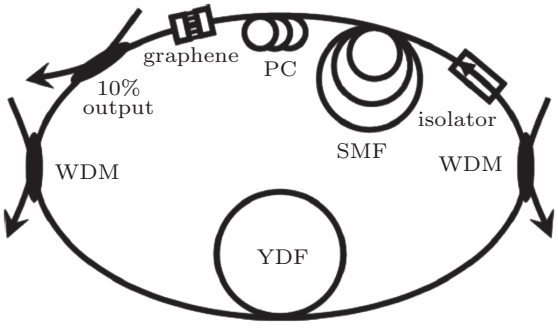


Fig. 14. Schematic diagram of a fiber laser. WDM, wavelength division multiplexer; YDF, ytterbium-doped fiber; SMF, single mode fiber; PC, polarization controller.[65]

It is found that a single layer of graphene absorbs about 2.3% of the light incident on it.[9] However, the absorption is saturated when the excited electrons and holes relax through the electron–hole recombination. Pauli blocking prevents electrons in the valence bands from being further excited. Mode-locking by graphene in the fiber laser[65] and the solid-state laser[66] has been successfully demonstrated. One interesting point is that with the Fermi level shifted by electrostatic gating, saturable absorption properties can be switched on and off. A schematic diagram of a fiber laser is shown in Fig. 14.

5.4. Optical polarizer

Polarizers, which convert a beam of light with undefined or mixed polarization into a beam with well defined polarization, are crucial passive components in optical systems. Current polarization controlling devices can be classified into sheet polarizers using anisotropic absorption media, prim polarizers by refraction, and Brewster-angle polarizers by reflection,[67] which are all bulky and difficult to integrate with photonic circuits. The in-line fiber polarizer is a promising alternative. In the conventional two-dimensional electron systems, only the transverse-magnetic mode can propagate. The spectra of electromagnetic modes are electron (hole) mass sensitive. Therefore, with massless Dirac fermions, graphene paints a radically new picture. By shifting the Fermi level, graphene can selectively support either the transverse-magnetic (TM) or transverse-electric (TE) electro-magnetic modes, which provides the basis for graphene polarizers that transform unpolarized incident light into polarized light.

Bao *et al.* fabricated an optical fiber polarizer with graphene as an in-line conductive layer.[68] A TE mode extinction ratio up to ~ 27 dB has been demonstrated, covering very broad communication bands. Millimeter-scale graphene with high continuity and uniformity is needed in this kind of device. A schematic diagram of the device is shown in Fig. 15.

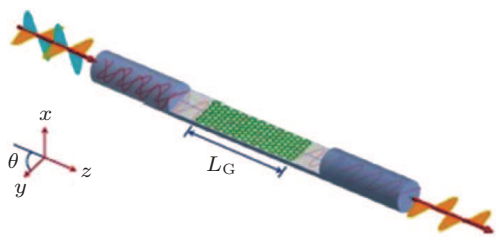


Fig. 15. Schematic model of fiber-to-graphene coupler based on a side-polished optical fiber, here L_G is the propagation distance (length of covered graphene film).[68]

6. Conclusions

In less than ten years, graphene has stimulated great interests in academic and industrial researches and become one of the most promising novel materials for beyond-CMOS technologies. Although, early on, the industrial interest was triggered by the high mobility of this material, it was quickly realized that the bandgap–mobility tradeoff inevitably constrains the applications of graphene for the conventional FET devices in digital applications. However, this shortcoming did not dampen the enthusiasm of the research community toward graphene electronics, as shown in this review. Aside from high mobility, graphene offers numerous other amazing electrical, optical, thermal, and mechanical properties that continually motivate innovations. In the history of science and engineering, few materials have attracted so much research effort and been subject to such rapid progress in such a short period of time. If the current progress continues, it is not impossible that some types of graphene-based electronic or optoelectronic devices/circuits may achieve enough functionality and maturity to be commercialized. Progress in the production of graphene is key to graphene commercialization. Researchers have been striving for large-scale graphene, which depends on material quality, defects, impurities induced in the transfer process, and other factors. Integration with other passive elements degrades graphene's performance, requiring much more efforts to optimize the graphene integration technology. It is likely that such breakthroughs may emerge in niche areas instead of mainstream digital electronics, e.g., analog electronics, optoelectronic components, contacts, interconnects, or even sensors.

References

[1] Novoselov K S, Geim A K, Morozov S V, Jiang D, Zhang Y, Dubonos S V, Grigorieval I V and Firsov A A 2004 *Science* **306** 666
[2] Lee C, Wei X D, Kysar J W and Hone J 2008 *Science* **321** 385
[3] Balandin A A 2011 *Nat. Mater.* **10** 569
[4] Bunch J S, Verbridge S S, Alden J S, Zande A M, Parpia J M, Craighead H G and McEuen P L 2008 *Nano Lett.* **8** 2458
[5] Morozov S V, Novoselov K S, Katsnelson M I, Schedin F, Elias D C, Jaszczak J A and Geim A K 2008 *Phys. Rev. Lett.* **100** 016602
[6] Wu Y, Jenkins K A, Valdes-Garcia A, Farmer D B, Zhu Y, Bol A A, Dimitrakopoulos C, Zhu W, Xia F, Avouris P and Lin Y M 2012 *Nano Lett.* **12** 3062
[7] Xia F, Farmer D B, Lin Y M and Avouris P 2010 *Nano Lett.* **10** 715
[8] Schwierz F and Pezoldt J 2012 *Solid-State and Integrated Circuit Technology (ICSICT) 2012 IEEE 11th International Conference on*
[9] Nair R R, Blake P, Grigorenko A N, Novoselov K S, Booth T J, Stauber T, Peres N M R and Geim A K 2008 *Science* **320** 1308
[10] Novoselov K S, Fal'ko V I, Colombo L, Gellert P R, Schwab M G and Kim K 2012 *Nature* **490** 192
[11] Geim A K and Novoselov K S 2007 *Nat. Mater.* **6** 183
[12] Schwierz F 2010 *Nat. Nanotech.* **5** 487
[13] Berger C, Song Z, Li T, Li X, Ogbazghi A Y, Feng R, Dai Z, Marchenkov A N, Conrad E H, First P N and Heer W A 2004 *J. Phys. Chem. B* **108** 19912

[14] Berger C, Song Z, Li X, Wu X, Brown N, Naud C, Mayou D, Li T, Hass J, Marchenkov A N, Conrad E H, First P N and Heer W A 2006 *Science* **312** 1191

[15] Deng P, Lei T, Lu J, Liu F, Zhang Y, Guo H, Zhang Y, Wang Y and Tang X 2013 *Chin. Phys. Lett.* **30** 018101

[16] Wang D, Zhang Y M, Lei T, Guo H, Wang R, Tang X and Wang H 2012 *Chin. Phys. B* **21** 038102

[17] Miao J, Huang L, Gao M, He J, Zhou H, Guo H, Tian Y, Zou Q, Zhang L, Zhang H, Wang Y, Du S, Zhou X, Castro N and Gao H J 2012 *Appl. Phys. Lett.* **100** 093101

[18] Kim K S, Zhao Y, Jang H, Lee S Y, Kim J M, Kim K S, Ahn J H, Kim P, Choi J Y and Hong B H 2009 *Nature* **457** 706

[19] Li X, Cai W, An J, Kim S, Nah J, Yang D, Piner R, Velamakanni A, Jung I, Tutuc E, Banerjee S K, Colombo L and Ruoff R S 2009 *Science* **324** 1312

[20] Wang W, Liang C, Li T, Yang H, Lu N and Wang Y 2013 *Chin. Phys. Lett.* **30** 028102

[21] Sutter P, Sadowski J T and Sutter E 2009 *Phys. Rev. B* **80** 245411

[22] Xiao K, Wu H, Lv H, Wu X and Qian H 2013 *Nanoscale* **5** 5524

[23] Gao L, Ren W, Xu H, Jin L, Wang Z, Ma T, Ma L, Zhang Z, Fu Q, Peng L M, Bao X and Cheng H 2012 *Nat. Commun.* **3** 699

[24] Li X, Zhu Y, Cai W, Borysiak M, Han B, Chen D, Piner R, Colombo L and Ruoff R S 2009 *Nano Lett.* **9** 4359

[25] Hsu A, Wang H, Shin Y C, Mailly B, Zhang X, Yu L, Shi Y, Lee Y H, Dubey M, Kim K K, Kong J and Palacios T 2013 *Proc. IEEE* **101** 1638

[26] Wu Y, Farmer D B, Xia F and Avouris P 2013 *Proc. IEEE* **101** 1620

[27] Cheng R, Bai J, Liao L, Zhou H, Chen Y, Liu L, Lin Y C, Jiang S, Huang Y and Duan X 2012 *Proc. Nat. Acad. Sci. USA* **109** 11588

[28] Lemme M C, Echtermeyer T J, Baus M and Kurz H 2007 *Electr. Dev. Lett. IEEE* **28** 282

[29] Meric I, Baklitskaya N, Kim P and Shepard K L 2008 *IEDM*

[30] Lin Y, Jenkins K A, Valdes-Garcia A, Small J P, Farmer D B and Avouris P 2008 *Nano Lett.* **9** 422

[31] Moon J S, Curtis D, Hu M, Wong D, McGuire C, Campbell P M, Jernigan G, Tedesco J L, VanMil B, Myers-Ward R, Eddy C and Gaskill D K 2009 *Electr. Dev. Lett.* **30** 650

[32] Lin Y M, Dimitrakopoulos C, Jenkins K A, Farmer D B, Chiu H Y, Grill A and Avouris P 2010 *Science* **327** 662

[33] Liao L, Lin Y, Bao M, Cheng R, Bai J, Liu Y, Qu Y, Wang K L, Huang Y and Duan X 2010 *Nature* **467** 305

[34] Wu Y, Lin Y, Bol A A, Jenkins K A, Xia F, Farmer D B, Zhu Y and Avouris P 2011 *Nature* **472** 74

[35] Robinson J A, LaBella M, Zhu M, Hollander M, Kasarda R, Hughes Z, Trumbull K, Cavalero R and Snyder D 2011 *Appl. Phys. Lett.* **98** 053103

[36] Mayorov A S, Gorbachev R V, Morozov S V, Britnell L, Jalil R, Ponomarenko L A, Blake P, Novoselov K S, Watanabe K, Taniguchi T and Geim A K 2011 *Nano Lett.* **11** 2396

[37] Lee B, Park S Y, Kim H, Cho K, Vogel E, Kim M, Wallace R and Kim J 2008 *Appl. Phys. Lett.* **92** 203102

[38] Meric I, Han M Y, Young A F, Ozyilmaz B, Kim P and Shepard K L 2008 *Nat. Nano.* **3** 654

[39] Rizzi L, Bianchi M, Behnam A, Carrion E, Guerriero E, Polloni L, Pop E and Sordan R 2012 *Nano Lett.* **12** 3948

[40] Han S, Jenkins K, Garcia A, Franklin A, Bol A and Haensch W 2011 *Nano Lett.* **11** 3690

[41] Guerriero E, Polloni L, Bianchi M, Behnam A, Carrion E, Rizzi L, Pop E and Sordan R 2013 *ACS Nano* **7** 5588

[42] Britnell L, Britnell L, Gorbachev R, Jalil R, Belle B, Schedin F, Mishchenko A, Georgiou T, Katsnelson M, Eaves L, Morozov S, Peres N, Leist J, Geim A K, Novoselov K S and Ponomarenko L A 2012 *Science* **335** 947

[43] Guerriero E, Polloni L, Rizzi L, Bianchi M, Mondello G and Sordan R 2012 *Small* **8** 357

[44] Wang H, Hsu A, Wu J, Kong J and Palacios T 2010 *Electr. Dev. Lett. IEEE* **31** 906

[45] Lin Y, Garcia A, Han S, Farmer D, Meric I, Sun Y, Wu Y, Dimitrakopoulos C, Grill A, Avouris P and Jenkins K 2011 *Science* **332** 1294

[46] Moon J S, Seo H, Antcliffe M, Le D, McGuire C, Schmitz A, Nyakiti L, Gaskill D, Campbell P, Lee K and Asbeck P 2013 *Electr. Dev. Lett. IEEE* **34** 465

[47] Maas S A 1987 *Microwave Theory and Techniques IEEE Transactions on* **35** 425

[48] Madan H, Hollander M J, LaBella M, Cavalero R, Snyder D, Robinson J A and Datta S 2012 *IEDM*

[49] Habibpour O, Cherednichenko S, Vukusic J, Yhland K and Stake J 2012 *Electr. Dev. Lett. IEEE* **33** 71

[50] Zhu W, Linghu C, Zhang J, Zhang L, and Yu Z 2012 *The International Conference on Simulation of Semiconductor Processes and Devices* (*SISPAD*)

[51] Lee S, Lee K, Liu C, Kulkarni G and Zhong Z 2012 *Nat. Commun.* **3** 1018

[52] Naeemi A and James D M 2009 *Electron Devices IEEE Transactions on* **56** 1822

[53] Chen X, Akinwande D, Lee K, Close G F, Yasuda S, Paul B C, Fujita S, Kong J and Wong H P 2010 *Electron Devices IEEE Transactions on* **57** 3137

[54] Xia F, Mueller T, Lin Y, Garcia A and Avouris P 2009 *Nat. Nano.* **4** 839

[55] Echtermeyer T J, Britnell L, Jasnos P K, Lombardo A, Gorbachev R V, Grigorenko A N, Geim A K, Ferrari A C and Novoselov K S 2011 *Nat. Commum.* **2** 458

[56] Kim K, Choi J Y, Kim T, Cho S H and Chung H J 2011 *Nature* **479** 338

[57] Pospischil A, Humer M, Furchi M, Guider R, Fromherz T and Mueller T 2013 arXiv:1302.3854

[58] Liu A S, Jones R, Liao L, Rubio D, Rubin D, Cohen O, Nicolaescu R and Paniccia M 2004 *Nature* **427** 615

[59] Liu J, Beals M, Pomerene A, Bernardis S, Sun R, Cheng J, Kimerling L C and Michell J 2008 *Nat. Photon* **2** 433

[60] Liu M, Yin X, Ulin-Avila E, Geng B, Zentgraf T, Ju L, Wang F and Zhang X 2011 *Nature* **474** 64

[61] Andersen D R 2010 *J. Opt. Soc. Am. B* **27** 818

[62] Liu X, Du D and Mourou G 1997 *IEEE J. Quantum Electron.* **33** 1706

[63] Drexler W, Morgner U, Kärtner F X, Pitris C, Boppart S A, Li X D, Ippen E P and Fujimoto J G 1999 *Opt. Lett.* **24** 1221

[64] Zhang H, Tang D, Knize R J, Zhao L, Bao Q and Loh K P 2010 *Appl. Phys. Lett.* **96** 111112

[65] Zhao L, Tang D, Zhang H, Wu X, Bao Q and Loh K P 2010 *Opt. Lett.* **35** 3622

[66] Tan W, Su C, Knize R, Xie G, Li L and Tang D 2010 *Appl. Phys. Lett.* **96** 031106

[67] Goldstein D 2003 *Polarized Light* (2nd edn)

[68] Bao Q, Zhang H, Wang B, Ni Z, Lim C, Wang Y, Yuan D, Tang D and Loh KP 2011 *Nat. Photo.* **5** 411